Chapter 6

Achievable Energy Efficiency and Spectral Efficiency of Large-Scale Distributed Antenna Systems

Wei Feng, Ning Ge and Jianhua Lu

Additional information is available at the end of the chapter

http://dx.doi.org/10.5772/66049

Abstract

In the large-scale distributed antenna system (LS-DAS), a large number of antenna elements are densely deployed in a distributed way over the coverage area, and all the signals are gathered at the cloud processor (CP) via dedicated fiber links for globally joint processing. Intuitively, the LS-DAS can inherit the advantage of both large-scale multiple-input-multiple-output (MIMO) and network densification; thus, it offers enormous gains in terms of both energy efficiency (EE) and spectral efficiency (SE). However, as the number of distributed antenna elements (DAEs) increases, the overhead for acquiring the channel state information (CSI) will increase accordingly. Without perfect CSI at the CP, which is the majority situation in practical applications due to limited overhead, the claimed gain of LS-DAS cannot be achieved. To solve this problem, this chapter considers a more practical case with only the long-term CSI including the path loss and shadowing known at the CP. As the long-term channel fading usually varies much more slowly than the short-term part, the system overhead can be easily controlled under this framework. Then, the EE-oriented and SE-oriented power allocation problems are formulated and solved by fractional programming (FP) and geometric programming (GP) theories, respectively. It is observed that the performance gain with only long-term CSI is still noticeable and, more importantly, it can be achieved with a practical system cost.

Keywords: large-scale distributed antenna system (LS-DAS), energy efficiency (EE), spectral efficiency (SE), long-term channel state information (CSI), fractional programming (FP), geometric programming (GP)

1. Introduction

The large-scale distributed antenna system (LS-DAS) is a promising candidate technology for the future 5G wireless network. In a LS-DAS, as shown in **Figure 1**, a large number of distributed antenna elements (DAEs) are densely scattered over the coverage area, and the signals from/to all the DAEs are gathered via dedicated fiber links, at the

cloud processor (CP), where the globally joint processing is performed [1, 2]. On one hand, the LS-DAS can be regarded as a special large-scale multiple-input-multiple-output (MIMO) system, as shown in **Figure 2**, with *distributed deployment of antenna elements*. On the other hand, it can be regarded as a special heterogeneous small-cell network, as shown in **Figure 3**, with *global inter-cell coordination*. As a consequence, the

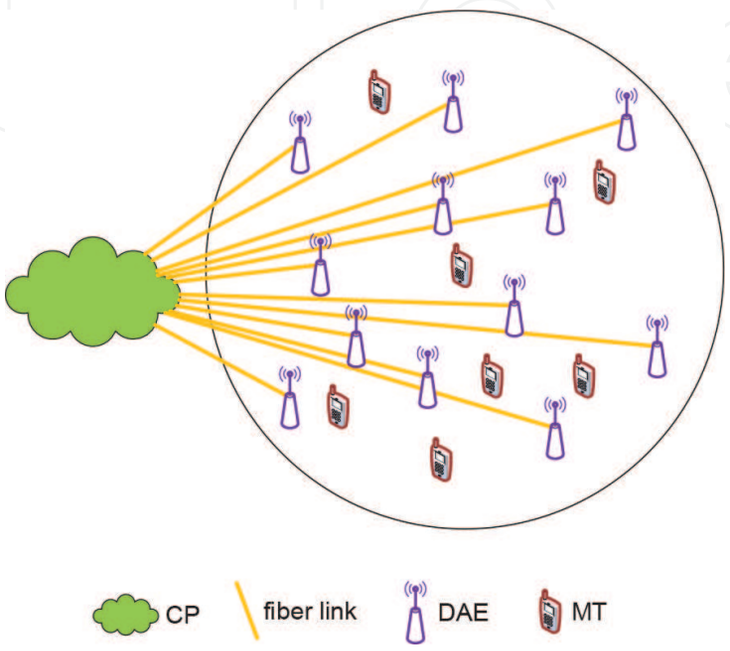

Figure 1. Illustration of a large-scale distributed antenna system.

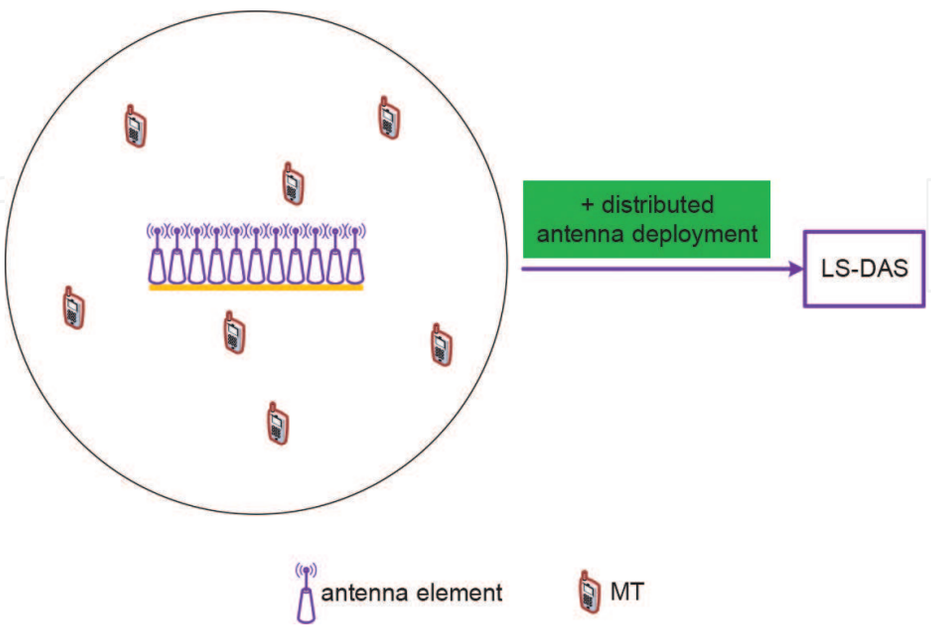

Figure 2. Illustration of a traditional large-scale MIMO system.

http://dx.doi.org/10.5772/66049

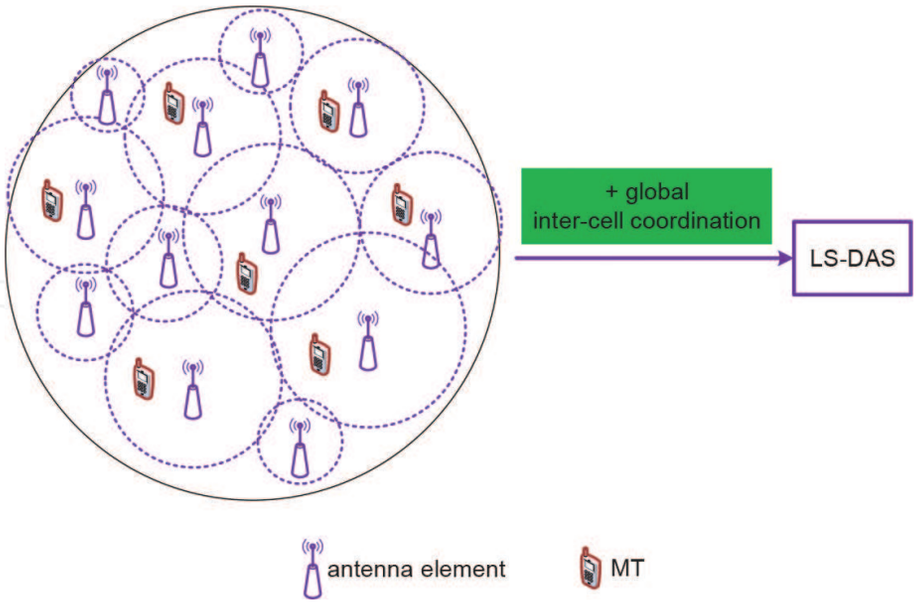

Figure 3. Illustration of a traditional heterogeneous small-cell network.

LS-DAS can inherit the advantage of both large-scale MIMO and network densification. Notably, existing studies have already shown that it can offer enormous gains in terms of both energy efficiency (EE) [3, 4] and spectral efficiency (SE) [5, 6].

Due to the distributed deployment of antenna elements, the average access distance of all the mobile terminals (MTs) is reduced. Moreover, due to the global coordination among all the DAEs, the multiplexing gain and diversity gain offered by multiple antenna elements can be obtained [7–9]. These are the main reasons for high EE and SE offered by a LS-DAS. However, to exploit the benefit of LS-DASs, the channel state information (CSI) is crucially required at the CP [10, 11]. Without perfect CSI, the interference among different DAEs will become intractable, and accordingly the system performance will be severely degraded.

In practical applications, the acquisition of full CSI would require an overwhelming amount of system overhead, including the training symbols for channel estimation, the system backhaul for CSI exchanging, and so on. Due to this point, in the literature, some researchers have shown that the system cost of CSI is quite an important issue for evaluating and designing multi-antenna systems. For example, in [12], it has been proved that the optimal number of transmit antennas is equal to the channel coherence interval (CCI). Thus, it will become useless to utilize more antennas than CCI under given channel dynamics. The authors of [13] particularly focused on the cost of CSI for network MIMO systems; they have shown that the optimal number of base stations that can be coordinated exists, which is mainly determined by the CCI in both time and frequency domains. Particularly, for the massive MIMO in frequency division duplex (FDD) mode, it is also very challenging to acquire full CSI at the base station side. In [14], a one-bit feedback scheme was proposed by using a set of predefined precoding vectors. The scheme only performs well in some specific cases, e.g., the multi-antenna channel following one-ring model.

In this chapter, we try to liberate the implementation of LS-DAS from the acquisition of full CSI. We note that the channel of a LS-DAS usually consists of path loss, shadowing, and Rayleigh fading [7–9]. Compared with Rayleigh fading, path loss and shadowing vary much more slowly and can be estimated in a much longer interval than CCI. Thus, it requires a controllable system overhead. In some of the existing studies, path loss and shadowing are classified as large-scale CSI [4, 6]. To distinguish from the *large-scale* in LS-DAS, for clarity, we here use long-term CSI to identify path loss and shadowing. With the knowledge of long-term CSI, the achievable EE and SE will be particularly investigated in the sequel. Different from the reported EE and SE with perfect CSI assumption, which actually cannot be achieved in most practice, our results can be approached with a limited system cost; thus, it is of great significance for the realistic implementation of LS-DASs.

In order to control the computational complexity at the CP, we first divide the whole system into a number of virtual cells (VCs) [5, 15]. As shown in **Figure 4**, the VC is established in a user-centric manner, i.e., each MT chooses only a subset of the surround DAEs for its data transmission. Then, each MT is served by its own VC under the interference from other VCs. To control the interference, the signals of all the VCs are designed in a coordinated fashion at the CP while maximizing the EE or SE of the system. Given VCs, the EE-oriented and the SE-oriented power allocation problems are formulated based on long-term CSI only, both of which are non-convex problems, and thus are difficult to solve. By adopting the fractional programming (FP) theory and the geometric programming (GP) theory, we propose two iterative power allocation algorithms. These algorithms can derive the locally optimal EE and SE of the system, respectively. It is further observed from the simulation results that the

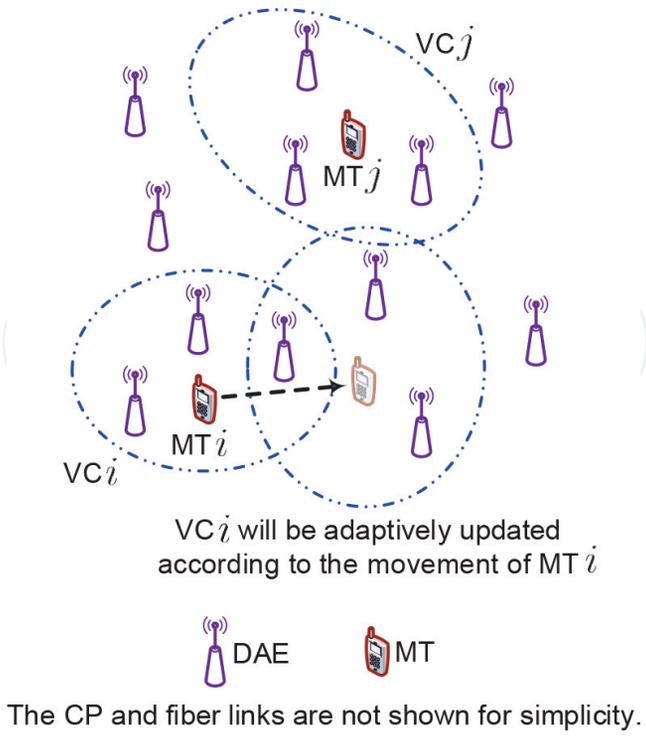

Figure 4. Illustration of VCs.

http://dx.doi.org/10.5772/66049

performance gain with only long-term CSI is still remarkable, while it can be achieved with a practical system cost.

The rest of this chapter is organized as follows. The system model of a multiuser LS-DAS is described in Section 2. In the subsequent Sections 3 and 4, the achievable EE and SE are discussed, respectively. Then, we show the simulation results to verify the superiority of the proposed schemes in Section 5. Finally, the conclusion of this chapter is drawn in Section 6.

Notations: $\mathbf{I}_n$ denotes an identity matrix with a dimension of n, and $\mathbf{O}$ is a zero matrix. $(.)^H$ represents the conjugate transpose operation. $\mathbb{C}^{M\times N}$ denotes the set of complex $M\times N$ matrices, and $\mathcal{CN}$ represents a complex Gaussian distribution. $\mathbf{E}_{(.)}$ represents the expectation operator, and $\mathrm{tr}(\cdot)$ represents the trace operator.

2. System Model

We consider a LS-DAS with K MTs. Without loss of generality, all the VCs consist of N DAEs, and the number of antenna elements equipped at each MT is M.

For MT k, the received signal is

$$\mathbf{y}^{(k)} = \mathbf{H}^{(k)}\mathbf{x}^{(k)} + \sum_{i=1,i\neq k}^{K} \mathbf{H}^{(k,i)}\mathbf{x}^{(i)} + \mathbf{n}^{(k)}, \tag{1}$$

where $\mathbf{H}^{(k)}\in\mathbb{C}^{M\times N}$, $k = 1,2,...,K$, represents the channel between the DAEs in VC k and MT k, $\mathbf{H}^{(k,i)}\in\mathbb{C}^{M\times N}$, $k = 1,2,...,K$, $i = 1,2,...,K$, denotes the channel between the DAEs in VC i and MT k, $\mathbf{x}^{(i)}\in\mathbb{C}^{N\times 1}$, $i = 1,2,...,K$, is the transmitted signal vector for MT i, and $\mathbf{n}^{(k)}\in\mathbb{C}^{M\times 1}$, $k = 1,2,...,K$, denotes the additive white Gaussian noise with distribution $\mathcal{CN}(0,\sigma^2 I_M)$.

$$\mathbf{E}\left[\mathbf{x}^{(k)}\mathbf{x}^{(k)^H}\right] = \mathbf{P}^{(k)} = \begin{bmatrix} p_1^{(k)} & & \\ & \ddots & \\ & & p_N^{(k)} \end{bmatrix},\ k = 1,...,K. \tag{2}$$

Assuming a total transmit power constraint $P_{\max}^{(k)}$ for MT k, we set

$$\sum_{n=1}^{N} p_n^{(k)} \leq P_{\max}^{(k)}. \tag{3}$$

The channel matrix can be modeled as

$$\mathbf{H}^{(k,i)} = \mathbf{S}^{(k,i)}\mathbf{L}^{(k,i)}, \tag{4}$$

where $\mathbf{S}^{(k,i)}$ and $\mathbf{L}^{(k,i)}$ reflect the short-term fading and the long-term fading, respectively. Particularly, the entries of $\mathbf{S}^{(k,i)}$ are all independent and identically distributed (i.i.d.) circular symmetric complex Gaussian variables following $\mathcal{CN}(0,1)$ distribution.

$$\mathbf{L}^{(k,i)} = \begin{bmatrix} l_1^{(k,i)} & & \\ & \ddots & \\ & & l_N^{(k,i)} \end{bmatrix}, \tag{5}$$

with

$$l_n^{(k,i)} = \sqrt{\left(D_n^{(k,i)}\right)^{-\gamma} S_n^{(k,i)}}, \quad n = 1, 2, ..., N, \tag{6}$$

where $D_n^{(k,i)}$ is the transmission distance between the DAE n in VC i and MT k, and γ is the path loss exponent, and $S_n^{(k,i)}$ represents the shadow fading caused by large objects such as tall buildings or walls.

3. Achievable Ee

Given perfect CSI, the authors of [16] have proposed an energy-efficient power allocation scheme for traditional DASs. In [17], further taking the inter-VC interference into consideration, an iterative power allocation scheme was presented to improve the EE of a LS-DAS, via applying the successive Taylor expansion method. In contrast, we investigate the achievable EE with the long-term CSI only in this section.

First of all, the sum rate of the system can be derived according to Eq. (1) as

$$R = \sum_{k=1}^{K} \log_2 \det\left(\mathbf{I}_M + \frac{\mathbf{H}^{(k)}\mathbf{P}^{(k)}\mathbf{H}^{(k)^H}}{\sigma_k^2}\right), \tag{7}$$

where

$$\sigma_k^2 = \sum_{i=1,\, i\neq k}^{K} \sum_{n=1}^{N} [l_n^{(k,i)}]^2 p_n^{(i)} + \sigma^2, \tag{8}$$

is the total interference-plus-noise power at MT k.

When only the long-term CSI is known, the average sum rate can be calculated via taking expectation over the short-term channel fading $\Omega = \{\mathbf{S}^{(k)} | k = 1,\ldots,K\}$ as

$$\overline{R} = \sum_{k=1}^{K} \mathbf{E}_{\Omega}\left[\log_2 \det\left(\mathbf{I}_M + \frac{\mathbf{H}^{(k)}\mathbf{P}^{(k)}\mathbf{H}^{(k)^H}}{\sigma_k^2}\right)\right]. \tag{9}$$

Then, the EE of the system, denoted as η, can be derived as

http://dx.doi.org/10.5772/66049

$$\eta = \frac{\overline{R}}{\rho \sum_{k=1}^{K} \sum_{n=1}^{N} p_n^{(k)} + P_c}, \tag{10}$$

where

$$\rho = \frac{\varepsilon}{\gamma}, \tag{11}$$

with ε and γ denoting the peak-to-average power ratio and the power amplifier efficiency, respectively, and P_c denotes the circuit power consumption [4].

In order to investigate the achievable EE under this framework, we formulate the following optimization problem:

$$\max \eta \tag{12a}$$

$$s.t. \sum_{n=1}^{N} p_n^{(k)} \le P_{\max}^{(k)}, \tag{12b}$$

$$p_n^{(k)} \ge 0, k = 1,\ldots, K, n = 1, \ldots, N. \tag{12c}$$

Because of the non-convexity of $\overline{R}$, the problem shown in Eq. (12) is a complicated non-convex problem [18]. To simplify it, we introduce an upper bound to the objective function as

$$\hat{\eta} = \frac{\sum_{k=1}^{K} \log_2 \det\left(\mathbf{I}_N + \frac{M\mathbf{P}^{(k)}\left(\mathbf{L}^{(k)}\right)^2}{\sigma_k^2}\right)}{\rho \sum_{k=1}^{K} \sum_{n=1}^{N} p_n^{(k)} + P_c}, \tag{13}$$

the numerator of which is an upper bound to $\overline{R}$ [10]. Accordingly, the problem in Eq. (12) can be reformulated as

$$\max \hat{\eta} \tag{14a}$$

$$s.t. \sum_{n=1}^{N} p_n^{(k)} \le P_{\max}^{(k)}, \tag{14b}$$

$$p_n^{(k)} \ge 0, \ k = 1,\ldots, K, n = 1, \ldots, N. \tag{14c}$$

which is simpler than Eq. (12). However, it is still non-convex [18]. To further solve the problem in Eq. (14), we express

$$\hat{\eta} = \frac{f_1 - f_2}{\rho \sum_{k=1}^{K} \sum_{n=1}^{N} p_n^{(k)} + P_c}, \tag{15}$$

where

$$f_1 = \sum_{k=1}^{K} \log_2 \det\left(\sigma_k^2 \mathbf{I}_N + M\mathbf{P}^{(k)}\mathbf{L}^{(k)2}\right), \tag{16a}$$

$$f_2 = \sum_{k=1}^{K} N \log_2(\sigma_k^2), \tag{16b}$$

both of which are clearly concave functions.

We find that if the numerator of $\hat{\eta}$, i.e., $f_1 - f_2$, can be transformed into a concave form, the problem in Eq. (14) can be recast as a quasi-concave fractional programming problem, further considering the linearity of its denominator [19]. Toward this end, we linearize f_2 by applying the first-order Taylor expansion at a given point $\overline{\mathbf{P}}$ as

$$\tilde{f}_2(\mathbf{P}|\overline{\mathbf{P}}) = \sum_{k=1}^{K} N \log_2\left(\sigma_k^2(\overline{\mathbf{P}})\right) + \log_2(e) \sum_{k=1}^{K} \frac{N}{\sigma_k^2(\overline{\mathbf{P}})} tr(G_k[\mathbf{P} - \overline{\mathbf{P}}]), \tag{17}$$

where $\mathbf{P} = \{\mathbf{P}^{(1)}, \ldots, \mathbf{P}^{(k)}\}$ and

$$\mathbf{G}_k = \text{diag}\{\mathbf{G}^{(k,1)}, \ldots, \mathbf{G}^{(k,K)}\}, \tag{18a}$$

$$\mathbf{G}^{(k,i)} = \left(\mathbf{L}^{(k,i)}\right)^2, k \neq i, k, i = 1, \ldots, K, \tag{18b}$$

$$\mathbf{G}^{(k,k)} = \mathbf{O}. \tag{18c}$$

By substituting $\tilde{f}_2(\mathbf{P}|\overline{\mathbf{P}})$ for $f_2(\mathbf{P})$, the problem in Eq. (14) can be approximated as

$$\max \overline{\eta} = \frac{f_1(\mathbf{P}) - \tilde{f}_2(\mathbf{P}|\mathbf{P})}{\rho \sum_{k=1}^{K} \sum_{n=1}^{N} p_n^{(k)} + P_c} \tag{19a}$$

$$s.t. \sum_{n=1}^{N} p_n^{(k)} \leq P_{\max}^{(k)}, \tag{19b}$$

$$p_n^{(k)} \geq 0, k = 1, \ldots, K, n = 1, \ldots, N, \tag{19c}$$

whose objective function is fortunately fractional with concave numerator and convex denominator [18]. Adopting the FP theory, the problem in Eq. (19) can be optimally solved in an iterative way. In our previous paper [4], we have shown in detail how to solve the problem in Eq. (19). In the following, for brevity, we just present the basic idea and procedure of the iterative algorithm.

We use $t \geq 1$ and $s \geq 1$ to denote the successive Taylor expansion iteration step and the FP iteration step, respectively. After introducing a positive variable ω, the following concave optimization problem can be formulated

$$\max v(\mathbf{P}|\mathbf{P}_{t-1,s-1},\omega) \tag{20a}$$

$$s.t. \sum_{n=1}^{N} p_n^{(k)} \leq P_{\max}^{(k)}, \tag{20b}$$

$$p_n^{(k)} \geq 0,\ k = 1, \ldots, K,\ n = 1, \ldots, N, \tag{20c}$$

where

$$v(\mathbf{P}|\mathbf{P}_{t-1,s-1},\omega) = f_1(\mathbf{P}) - \tilde{f}_2(\mathbf{P}|\mathbf{P}_{t-1,s-1}) - \omega\rho \sum_{k=1}^{K}\sum_{n=1}^{N} p_n^{(k)} - \omega P_c. \tag{21}$$

Further define

$$V(\omega) = \max v(\mathbf{P}|\mathbf{P}_{t-1,s-1},\omega), \tag{22}$$

Algorithm 1 Iterative power allocation for maximizing EE.

---

1. Initialization: $\mathbf{P}_0 = \mathbf{diag}\{\mathbf{P}_0^{(1)},\cdots,\mathbf{P}_0^{(K)}\}$ with $\mathbf{P}_0^{(k)} = \frac{\mathbf{P}_{\max}^{(k)}}{N}\mathbf{I}_N$, $k = 1, \ldots, K$, $\mathbf{P}_{0,0}^{(k)} = \mathbf{P}_0^{(k)}$, $k = 1, \ldots, K$, $\omega = 0$, and $\xi = 1 \times 10^{-3}$, $\delta = 1 \times 10^{-3}$, $t = 1, s = 1$;
2. Solve Eq. (20), and denote the obtained power matrix by $\mathbf{P}_{0,1}^{(k)}$, $k = 1, \ldots, K$, set $\mathbf{P}_1^{(k)} = \mathbf{P}_{0,1}^{(k)}$, $k = 1, \ldots, K$, and $\mathbf{P}_1 = \mathbf{diag}\{\mathbf{P}_1^{(1)},\cdots,\mathbf{P}_1^{(K)}\}$;
3. **while** $|\hat{\eta}(\mathbf{P}_t) - \hat{\eta}(\mathbf{P}_{t-1})|/\hat{\eta}(\mathbf{P}_{t-1}) > \xi$ **do**
4. $t = t + 1$, $s = 1$, and $\omega = 0$;
5. $\mathbf{P}_{t-1,0}^{(k)} = \mathbf{P}_{t-1}^{(k)}$, $k = 1, \ldots, K$;
6. Solve Eq. (20), derived $V(\omega)$ and denote the obtained power matrix by $\mathbf{P}_{t-1,1}^{(k)}$, $k = 1, \ldots, K$;
7. **while** $V(\omega) > \delta$ **do**
8. $\omega = \overline{\eta}\left(\mathbf{P}_{t-1,s}^{(k)}|\mathbf{P}_{t-1}^{(k)}\right)$;
9. $s = s + 1$;
10. Solve Eq. (20), derived $V(\omega)$ and denote the obtained power matrix by $\mathbf{P}_{t-1,s}^{(k)}$, $k = 1, \ldots, K$;
11. **end while**

12. $\mathbf{P}_t^{(k)} = \mathbf{P}_{t-1,s}^{(k)}$, $k = 1, ...,K$, and $\mathbf{P}_t = \text{diag}\{\mathbf{P}_t^{(1)},\cdots,\mathbf{P}_t^{(K)}\}$;

13. end while

14. Output: $\mathbf{P}_t$.

we can propose an iterative power allocation algorithm for maximizing EE, as described in **Algorithm 1**. By adopting **Algorithm 1**, the achievable EE with long-term CSI only can be derived with low computational complexity [4].

4. Achievable Se

For traditional single-cell DASs, the achievable SE was studied in [20, 21], which by considering the general DAS with random antenna layout has identified that DAS outperforms colocated multi-antenna systems. In [22], the authors have taken the inter-cell interference into consideration, and they have presented a close-form expression for the achievable EE in a multi-cell environment. However, this work has not considered interference coordination. The authors of [23] took a step further; they have put forward a coordinated power allocation scheme for dealing with the inter-cell interference. Nevertheless, the result was derived by approximately treating the inter-cell interference as Gaussian noise, and thus it is only applicable to the low signal-to-noise-ratio (SNR) situation. In a recent work, the SE of single-cell multiuser LS-DAS was studied [24]. It however also has not considered interference coordination, which is in general inevitable in most practical applications. Different from all the above existing studies, in this section, we investigate the achievable SE of a LS-DAS with long-term CSI only.

With the target of average system sum rate maximization, the problem of SE-oriented power allocation can be formulated as

$$\max \ \overline{R} \tag{23a}$$

$$s.t. \ \sum_{n=1}^{N} p_n^{(k)} \leq P_{\max}^{(k)}, \tag{23b}$$

$$p_n^{(k)} \geq 0, \ k = 1, ..., K, \ n = 1, ...,N. \tag{23c}$$

As $\overline{R}$ is non-convex, this problem is complicatedly non-convex [18]. Besides, the objective function is actually in an integral form as a result of the expectation operator in $\overline{R}$, and it cannot be directly expressed in a compact closed form, which renders it even more challenging to obtain the optimal solution of Eq. (23).

We try to simplify the formulated problem. To this end, a closed-form approximation for the average system sum rate $\overline{R}$ is leveraged as

http://dx.doi.org/10.5772/66049

$$\overline{R}_{ap} = \sum_{k=1}^{K}\sum_{n=1}^{N}\log_2\left(1+\frac{[l_n^{(k)}]^2 p_n^{(k)}\Upsilon_k^{-1}M}{\sigma_k^2}\right) + M\sum_{k=1}^{K}\log_2(\Upsilon_k) - M\sum_{k=1}^{K}\log_2 e(1-\Upsilon_k^{-1}), \tag{24}$$

where Υ_k satisfies

$$\Upsilon_k = 1+\sum_{n=1}^{N}\frac{[l_n^{(k)}]^2 p_n^{(k)}}{\sigma_k^2+[l_n^{(k)}]^2 p_n^{(k)}\Upsilon_k^{-1}M},\ k=1,..,K. \tag{25}$$

This approximation can be derived through using the random matrix theory [10], and the introduced parameter Υ_k can be calculated in an iterative way as shown in the following **Algorithm 2**.

According to the existing studies [10], $\overline{R}_{ap}$ is quite a precise approximation for $\overline{R}$. Therefore, we directly use it as the objective function, and the joint power allocation problem can be recast as

$$\max\ \overline{R}_{ap} \tag{26a}$$

$$s.t.\ \sum_{n=1}^{N} p_n^{(k)} \le P_{\max}^{(k)}, \tag{26b}$$

$$p_n^{(k)} \ge 0,\ k=1,...,K,\ n=1,...,N, \tag{26c}$$

which is much simplified. However, due to the non-convexity of $\overline{R}_{ap}$ [18], the new problem in Eq. (26) is still non-convex. In the following, we explore the achievable SE of the system by contriving an iterative algorithm, which can find a locally optimal solution of Eq. (26) efficiently.

To eliminate the effect of the introduced parameters Υ_1, Υ_2, ..., Υ_K, we first fix Υ_1, Υ_2, ..., Υ_K as constants. Then we can equivalently simplify the objective function in Eq. (26) as

$$\overline{R}'_{ap} = \sum_{k=1}^{K}\sum_{n=1}^{N}\log_2\left(1+\frac{[l_n^{(k)}]^2 p_n^{(k)}\Upsilon_k^{-1}M}{\sigma_k^2}\right). \tag{27}$$

As $\log_2(\cdot)$ is monotonically increasing, the problem shown in Eq. (26) can be equivalently transformed into

$$\min\ \prod_{k=1}^{K}\prod_{n=1}^{N}\frac{\sigma_k^2}{\sigma_k^2+[l_n^{(k)}]^2 p_n^{(k)}\Upsilon_k^{-1}M} \tag{28a}$$

$$s.t.\ \sum_{n=1}^{N} p_n^{(k)} \le P_{\max}^{(k)}, \tag{28b}$$

$$p_n^{(k)} \geq 0,\ k = 1, ..., K,\ n = 1, ..., N. \tag{28c}$$

Define

$$f_{n,k}(\mathbf{P}) = \sigma_k^2(\mathbf{P}) + [l_n^{(k)}]^2 p_n^{(k)} \Upsilon_k^{-1} M = \sum_{i=1, i\neq kj=1}^{K} \sum^{N} g_j^{(k,i)}(\mathbf{P}) + g_n^{(k)}(\mathbf{P}) + \sigma^2, \quad n = 1, ..., N, k = 1, ..., K, \tag{29}$$

where

$$g_j^{(k,i)}(\mathbf{P}) = [l_j^{(k,i)}]^2 p_j^{(i)},\ k \neq i, \tag{30}$$

$$g_n^{(k)}(\mathbf{P}) = [l_n^{(k)}]^2 p_n^{(k)} \Upsilon_k^{-1} M, \tag{31}$$

and then, given a feasible point $\overline{\mathbf{P}}$, an approximation of $f_{n,k}(\mathbf{P})$ can be obtained as

$$\tilde{f}_{n,k}(\mathbf{P}|\overline{\mathbf{P}}) = \left(\prod_{i=1, i\neq kj=1}^{K} \prod^{N} \left(\frac{g_j^{(k,i)}(\mathbf{P})}{\alpha_{n,j}^{(k,i)}} \right)^{\alpha_{n,j}^{(k,i)}} \right) \times \left(\frac{g_n^{(k)}(\mathbf{P})}{\alpha_{n,n}^{(k)}} \right)^{\alpha_{n,n}^{(k)}} \times \left(\frac{\sigma^2}{\alpha_{n,k}^0} \right)^{\alpha_{n,k}^0}, \tag{32}$$

where

$$\alpha_{n,j}^{(k,i)} = g_j^{(k,i)}(\overline{\mathbf{P}}) / f_{n,k}(\overline{\mathbf{P}}), \tag{33}$$

$$\alpha_{n,n}^{(k)} = g_n^{(k)}(\mathbf{P}) / f_{n,k}(\overline{\mathbf{P}}), \tag{34}$$

$$\alpha_{n,k}^0 = \sigma^2 / f_{n,k}(\overline{\mathbf{P}}). \tag{35}$$

By using the inequality of arithmetic and geometric means, it is easy to obtain that

$$f_{n,k}(\mathbf{P}) \geq \tilde{f}_{n,k}(\mathbf{P}|\overline{\mathbf{P}}). \tag{36}$$

The equality holds if and only if

$$\mathbf{P} = \overline{\mathbf{P}}. \tag{37}$$

By replacing $f_{n,k}(\mathbf{P})$ with $\tilde{f}_{n,k}(\mathbf{P}|\overline{\mathbf{P}})$, the problem in Eq. (28) can be recast as

$$\min \prod_{k=1n=1}^{K} \prod^{N} \frac{\sigma_k^2}{\tilde{f}_{n,k}}(\mathbf{P}) \tag{38a}$$

$$s.t. \sum_{n=1}^{N} p_n^{(k)} \leq P_{\max}^{(k)}, \tag{38b}$$

$$p_n^{(k)} \geq 0,\ k = 1, ..., K,\ n = 1, ..., N, \tag{38c}$$

which is a good approximation for the original problem in the neighborhood of $\overline{\mathbf{P}}$. More importantly, it is a standard GP problem [25]; thus, it can be efficiently solved via convex optimization tools, e.g., the interior point algorithm [18].

We use $t \geq 1$ and $s \geq 1$ to denote the updating iteration step of Υ_k and the arithmetic-to-geometric approximation iteration step, respectively. Then the following convex optimization problem is derived

$$\min \prod_{k=1}^{K} \prod_{n=1}^{N} \frac{\sigma_k^2}{\tilde{f}_{n,k}} (\mathbf{P} | \mathbf{P}^{s-1}, \Upsilon_k^t) \tag{39a}$$

$$s.t. \sum_{n=1}^{N} p_n^{(k)} \leq P_{\max}^{(k)}, \tag{39b}$$

$$p_n^{(k)} \geq 0, k = 1, ..., K, n = 1, ..., N. \tag{39c}$$

Accordingly, we propose an iterative power allocation algorithm for maximizing SE as described in **Algorithm 2**. In the algorithm, $\Upsilon_k, k = 1, ..., K$ and $\mathbf{P}$ are updated in an alternate way. By adopting the algorithm, the achievable SE with long-term CSI only can be derived with low computational complexity [6].

5. Simulation Results

In this section, we illustrate the EE and SE performance of the proposed schemes by simulations. To be general, we consider a circular coverage area with a radius of 500 m. There are 20 DAEs randomly deployed in the coverage area with a two-dimension uniform distribution. The number of MTs is set as $K = 3$. The number of antenna elements equipped at each MT is set as $M = 3$. In order to fully exploit the spatial degree of freedom of each MT and, in the meantime, well control the system complexity, we set the size of each VC as $N = M = 3$. As for the channel parameters, we set $\gamma = 4$ (path loss exponent), $\sigma^2 = -107$ dBm (noise power), and the shadowing standard deviation is 8 dB. Without loss of generality, we consider the same transmit power constraint for all MTs, i.e., $P_{\max}^{(1)} = P_{\max}^{(2)} = P_{\max}^{(3)}$. Particularly, 100 randomly selected system topologies are considered in the simulation, and the averaged results are shown in the following.

First, the achievable EE of different schemes is compared in **Figure 5**. Both the scheme presented in reference [16] and the simplest equal power allocation scheme are considered. It can be seen from **Figure 5** that the proposed scheme outperforms the other ones, especially when the transmit power constraint goes larger. The scheme proposed in [16] has not considered interference coordination; thus, in a multi-VC setting, its performance is worse than the proposed scheme, although it has assumed the perfect CSI as the CP. In contrast, although using the long-term CSI only, the proposed scheme can still offer the highest EE performance. We can also observe from **Figure 5** that the key point for high EE is to set proper transmit power, i.e., when the transmit power has reached a corresponding point, it should no longer be

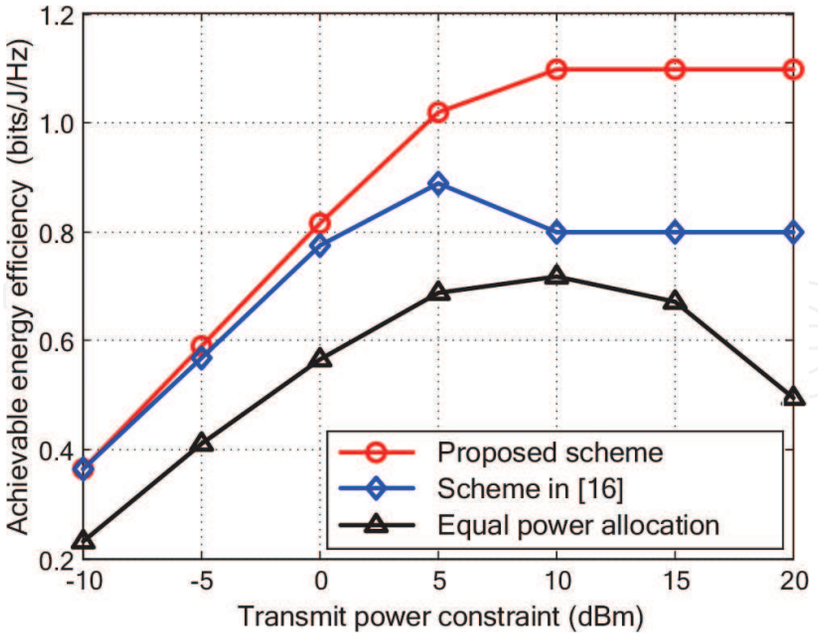

Figure 5. Comparison of achievable EE by different schemes.

increased even though the power consumption constraint goes larger. Intuitively, this observation can be explained by the fact that when the transmit power goes larger, the sum rate gain will become smaller and smaller due to the impact of interference; thus, the EE of the scheme will fall instead of rising.

Algorithm 2 Iterative power allocation for maximizing SE.

1. Initialization: Set $\mathbf{P}^0 = \{[p_1^{(1)}]^0, [p_2^{(1)}]^0, ..., [p_N^{(K)}]^0\}$, where $[p_n^{(k)}]^0 = \frac{P_{\max}^{(k)}}{N}$, $k = 1, ..., K$, $n = 1, ..., N$, and $\varepsilon = 1 \times 10^{-4}$, $\delta = 1 \times 10^{-3}$, $s = 1$;
2. **for** $k = 1$ to K **do**
3. $t = 1$;
4. $\Upsilon_k^0 = 1$;
5. $\Upsilon_k^1 = 1 + \sum_{n=1}^{N} \frac{[l_n^{(k)}]^2 [p_n^{(k)}]^0}{\sigma_k^2(\mathbf{P}^0) + [l_n^{(k)}]^2 [p_n^{(k)}]^0 [\Upsilon_k^0]^{-1} M}$;
6. **while** $|\Upsilon_k^t - \Upsilon_k^{t-1}| > \varepsilon$ **do**
7. $t = t + 1$;
8. $\Upsilon_k^t = 1 + \sum_{n=1}^{N} \frac{[l_n^{(k)}]^2 [p_n^{(k)}]^0}{\sigma_k^2(\mathbf{P}^0) + [l_n^{(k)}]^2 [p_n^{(k)}]^0 [\Upsilon_k^{t-1}]^{-1} M}$;
9. **end while**
10. Output $\Upsilon_k' = \Upsilon_k^t, k = 1, ..., K$.
11. **end for**

12. Solve Eq. (39) with $\Upsilon_k = \Upsilon_k^{'}, k = 1, ..., K$, and denote the obtained power matrix by $\mathbf{P}^1$;

13. **while** $|\overline{R}_{ap}(\mathbf{P}^s) - \overline{R}_{ap}(\mathbf{P}^{s-1})| / \overline{R}_{ap}(\mathbf{P}^{s-1}) > \delta$ **do**

14. **for** $k = 1$ to K **do**

15. $t = 1$;

16. $\Upsilon_k^0 = 1$;

17. $\Upsilon_k^1 = 1 + \sum_{n=1}^{N} \frac{[l_n^{(k)}]^2 [p_n^{(k)}]^s}{\sigma_k^2(\mathbf{P}^s) + [l_n^{(k)}]^2 [p_n^{(k)}]^s [\Upsilon_k^0]^{-1} M}$;

18. **while** $|\Upsilon_k^t - \Upsilon_k^{t-1}| >$ **do**

19. $t = t + 1$;

20. $\Upsilon_k^t = 1 + \sum_{n=1}^{N} \frac{[l_n^{(k)}]^2 [p_n^{(k)}]^s}{\sigma_k^2(\mathbf{P}^s) + [l_n^{(k)}]^2 [p_n^{(k)}]^s [\Upsilon_k^{t-1}]^{-1} M}$;

21. **end while**

22. Output $\Upsilon_k^{'} = \Upsilon_k^t, k = 1, ..., K$.

23. **end for**

24. $s = s + 1$;

25. Solve Eq. (39) with $\Upsilon_k = \Upsilon_k^{'}, k = 1, ..., K$, and denote the obtained power matrix by26: $\mathbf{P}^s$;

26. **end while**

27. Output: $\mathbf{P}^s$.

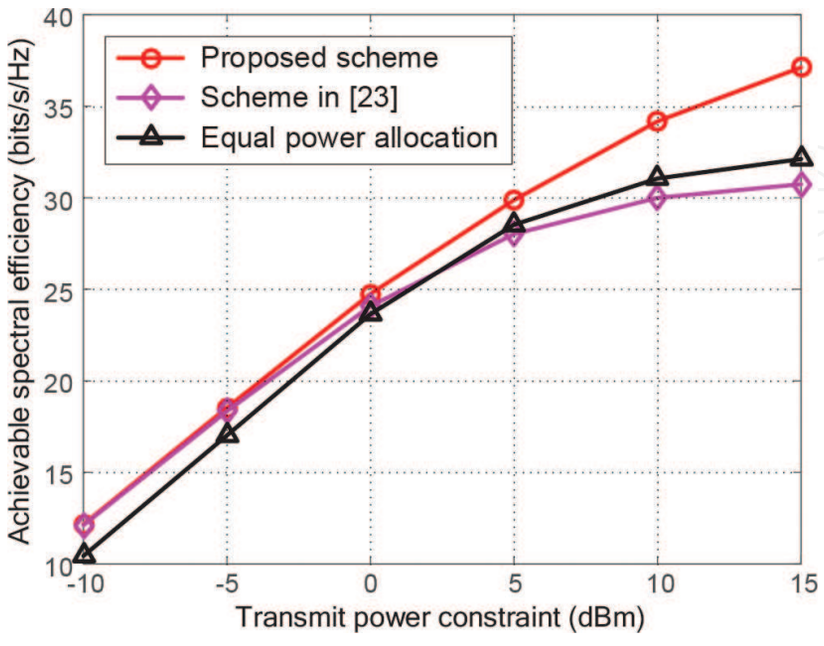

Figure 6. Comparison of achievable SE by different schemes.

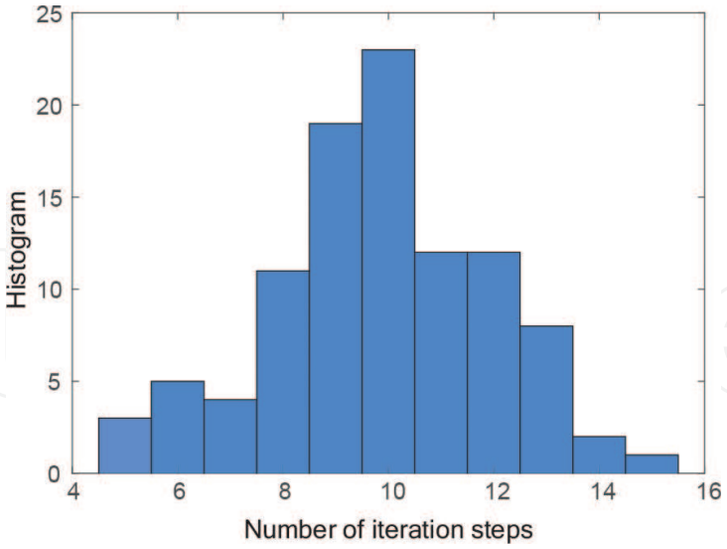

Figure 7. Histogram of the number of iteration steps for **Algorithm 1**.

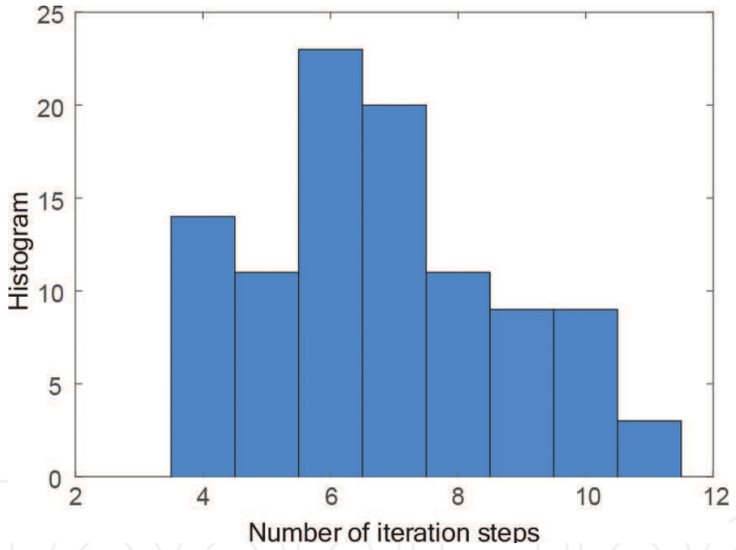

Figure 8. Histogram of the number of iteration steps for **Algorithm 2**.

Then, we evaluate the performance of the proposed scheme in terms of achievable SE. The scheme presented in reference [23] and equal power allocation scheme are taken into comparison. The results are shown in **Figure 6**. We can find that the proposed scheme performs the best among the three schemes. The scheme presented in [23] is only applicable to the low SNR condition; thus, the performance gas between it and the proposed scheme goes larger when the transmit power constraint increases, which implies that the impact of inter-VC interference becomes bigger. The results identify that it is still effective for enhancing the SE of the system when only the long-term CSI is available.

http://dx.doi.org/10.5772/66049

According to the discussion in [4, 6], the proposed **Algorithms 1** and **2** are assured to converge to a local optimum. The histogram of the number of iteration steps is illustrated in **Figures 7** and **8**, for **Algorithms 1** and **2**, respectively. We can observe from the figures that 15 iteration steps are enough for the convergence of **Algorithm 1** and that for **Algorithm 2** is 11.

6. Conclusions

The LS-DAS is a promising candidate technology for the future 5G wireless network, due to its remarkable gains in terms of both EE and SE. In this chapter, we try to liberate the implementation of LS-DAS from the acquisition of full CSI. With the knowledge of long-term CSI, including the path loss and shadow fading, the achievable EE and SE have been investigated. Different from the reported EE and SE with perfect CSI condition, which actually cannot be achieved in most practice, our results can be achieved with a limited system cost; thus, it is of great significance for the realistic implementation of LS-DASs. We also use the concept of VC to control the computational complexity at the CP. Accordingly, we design the transmit power of all the VCs in a coordinated fashion, to control the interference and finally maximize EE or SE of the system. Particularly, the EE-oriented and the SE-oriented power allocation problems are formulated based on long-term CSI only, both of which are non-convex problems, and thus are difficult to solve. By adopting the FP theory and the GP theory, we propose two iterative power allocation algorithms. These algorithms can derive the locally optimal EE and SE of the system, respectively. It is further observed from the simulation results that the performance gain with only long-term CSI is still remarkable, while it can be achieved with a practical system overhead.

Acknowledgements

This work was supported in part by the National Science Foundation of China for Young Scholars under grant no. 61201186 and the National Basic Research Program of China under grant no. 2013CB329001 and the National Science Foundation of China under grant no. 61132002.

Author details

Wei Feng*, Ning Ge and Jianhua Lu

*Address all correspondence to: fengw@mails.tsinghua.edu.cn

Department of Electronic Engineering, Tsinghua National Laboratory for Information Science Technology, Tsinghua University, Beijing, PR China

References

[1] Dai L. A comparative study on uplink sum capacity with co-located and distributed antennas. IEEE Journal on Selected Areas in Communications. 2011;29:1200–1213. DOI:10.1109/JSAC.2011.110608

[2] Feng W, Chen Y, Shi R, Ge N, and Lu J. Exploiting macro-diversity in massively distributed antenna systems: a controllable coordination perspective. IEEE Transactions on Vehicular Technology. DOI:10.1109/TVT.2015.2506720

[3] Feng W, Chen Y, Ge N, and Lu J. Optimal energy-efficient power allocation for distributed antenna systems with imperfect CSI. IEEE Transactions on Vehicular Technology. 2016;65:7759–7763. DOI:10.1109/TVT.2015.2497140

[4] Wang J, Feng W, Chen Y, and Zhou S. Energy efficient power allocation for multicell distributed antenna systems. IEEE Communications Letters. 2016;20:177–180. DOI:10.1109/LCOMM.2015.2498608

[5] Wang J and Dai L. Downlink rate analysis for virtual-cell based large-scale distributed antenna systems. IEEE Transactions on Wireless Communications. 2016;15:1998–2011. DOI:10.1109/TWC.2015.2497678

[6] Wang Y, Feng W, Zhao Y, Zhou S, and Wang J. Joint power allocation for multi-cell distributed antenna systems with large-scale CSIT. In: Proceedings of the IEEE International Conference on Communications (ICC'12); 10–15 June 2012; Ottawa. IEEE; 2012. pp. 6786–6791.

[7] Roh W, Paulraj A. Outage performance of the distributed antenna systems in a composite fading channel. In: Proceedings of the IEEE Vehicular Technology Conference (VTC 2002-Fall); September 2002; Vancouver. IEEE; 2002. pp. 1520–1524.

[8] Roh W, Paulraj A. MIMO channel capacity for the distributed antenna systems. In: Proceedings of the IEEE Vehicular Technology Conference (VTC 2002-Fall); September 2002; Vancouver. IEEE; 2002. pp. 706–709.

[9] Feng W, Li Y, Gan J, Zhou S, Wang J, and Xia M. On the deployment of antenna elements in generalized multi-user distributed antenna systems. Mobile Networks and Applications. 2011;16:35–45. DOI:10.1007/s11036-009-0214-1

[10] Feng W, Wang Y, Ge N, Lu J, and Zhang J. Virtual MIMO in multi-cell distributed antenna systems: coordinated transmissions with large-scale CSIT. IEEE Journal on Selected Areas in Communications. 2013;31:2067–2081. DOI:10.1109/JSAC.2013.131009

[11] Wang Y, Feng W, Xiao L, Zhao Y, and Zhou S. Coordinated multicell transmission for distributed antenna systems with partial CSIT. IEEE Communications Letters. 2012;16:1044–1047. DOI:10.1109/LCOMM.2012.050912.120383

[12] Hassibi B, Hochwald BM. How much training is needed in multiple-antenna wireless links? IEEE Transactions on Information Theory. 2003;49:951–963. DOI: 10.1109/TIT.2003.809594

[13] Caire G, Ramprashad SA, and Papadopoulos HC. Rethinking network MIMO: Cost of CSIT, performance analysis, and architecture comparisons. In: Proceedings of the Information Theory and Applications Workshop (ITA'10); 31 January–5 February 2010; San Diego. IEEE; 2010. pp. 1–10.

[14] Zhang Y, Feng W, and Ge N. Dealing with large overhead in FDD massive MIMO systems: a one-bit feedback scheme. In: Proceedings of International Conference on Telecommunications (ICT'16); 16–18 May 2016; Thessaloniki. IEEE; 2016. pp. 1–5.

[15] Feng W, Ge N, and Lu J. Hierarchical transmission optimization for massively dense distributed antenna systems. IEEE Communications Letters. 2015;19:673–676. DOI:10.1109/LCOMM.2015.2401584

[16] Chen X, Xu X, and Tao X. Energy efficient power allocation in generalized distributed antenna system. IEEE Communications Letters. 2012;16:1022–1025. DOI:10.1109/LCOMM.2012.051512.120241

[17] Wang J, Wang Y, Feng W, Su X, and Zhou S. An iterative power allocation scheme for improving energy efficiency in massively dense distributed antenna systems. In: Proceedings of the IEEE Vehicular Technology Conference (VTC Spring'16); 15–18 May 2016; Nanjing. IEEE; 2016. pp. 1–5.

[18] Boyd S, Vandenberghe L, Convex Optimization. New York: Cambridge University; 2004. 730 p. ISBN:0 521 83378 7

[19] Dinkelbach W. On nonlinear fractional programming. Management Science. 1967;13:492–498. DOI:10.1287/mnsc.13.7.492

[20] Zhuang H, Dai L, Xiao L, and Yao Y. Spectral efficiency of distributed antenna systems with random antenna layout. Electronics Letters. 2003;39:495–496. DOI:10.1049/el:20030327

[21] Feng W, Zhang X, Zhou S, Wang J, and Xia M. Downlink power allocation for distributed antenna systems with random antenna layout. In: Proceedings of the IEEE Vehicular Technology Conference (VTC Fall'09); 20–23 September 2009; Anchorage. IEEE; 2009. pp. 1–5.

[22] Choi W, Andrews JG. Downlink performance and capacity of distributed antenna systems in a multicell environment. IEEE Transactions on Wireless Communications 2007;6:69–73. DOI:10.1109/TWC.2007.05207

[23] Feng W, Wang Y, Zhao M, Zhou S, and Wang J. Practical power allocation for clustered distributed antenna systems in the low SNR regime. AEU - International Journal of Electronics and Communications 2010;65:595–598. DOI:10.1016/j.aeue.2010.07.005

[24] Li J, Wang D, Zhu P, and You X. Spectral efficiency analysis of single-cell multi-user large-scale distributed antenna system. IET Communications 2014;8:2213–2221. DOI:10.1049/iet-com.2013.0855

[25] Boyd SP, Kim SJ, Hassibi A, and Vandenbarghe L. A tutorial on geometric programming. Optimization and Engineering. 2007;8:67–128. DOI: 10.1007/s11081-007-9001-7

IntechOpen